IIETA International Information and Engineering Technology Association
Advancing the World of Information and Engineering

Traitement du Signal
Vol. 42, No. 1, February, 2025, pp. 11-18
Journal homepage: http://iieta.org/journals/ts

Enhancement for Astronomical Low-Resolution Images Using Discrete-Stationary Wavelet Transforms and New Edge-Directed Interpolation

Wasnaa Witwit[1*], Huda Hallawi[2], Yifan Zhao[3]

[1] Department of Physics, College of Science, University of Babylon, Babel 51001, Iraq
[2] Department of Information Technology, College of Computer Science and Information Technology, University of Kerbala, Kerbala 51001, Iraq
[3] Through-life Engineering Services Institute, Cranfield Manufacturing, Cranfield University, Cranfield MK43 0AL, UK

Corresponding Author Email: sci.wasnaa.jaafar@uobabylon.edu.iq

https://doi.org/10.18280/ts.420102

Received: 20 April 2024
Revised: 2 August 2024
Accepted: 4 December 2024
Available online: 28 February 2025

Keywords:
Discrete Wavelet Transform (DWT), Stationary Wavelet Transform (SWT), New Edge-directed Interpolation (NEDI), resolution enhancement, super-resolution, astronomical images

ABSTRACT

The physical resolution of astronomic imaging appliances, characterised as device parameters and physical effects, provides a chance for resolution enhancement methods. The proposed paper comes up with an enhanced technique for improving the image spatial resolution by merging three techniques which are Discrete Wavelet Transform (DWT) and Stationary Wavelet Transform (SWT) combined with an algorithm called New Edge-directed Interpolation (NEDI). The spatial resolution is enriched within the new approach by retrieving the missing edge elements due to the restrictions of imaging devices for astronomical noisy low-resolution (LR) images. The image of LR is divided to sub-bands of low and high frequencies (LF, HF) using (SWT) and (DWT), and thereafter the HF sub-bands of DWT are interpolated by NEDI. For enhancing the assessed high sub-bands, the HF of SWT is added to the interpolated HF of DWT. For maintaining better edge details and addressing the noise artefacts in the modified wavelet coefficients, the new high sub-bands are handled through NEDI and an adaptive threshold operation. Finally, for retrieving an image of a high resolution, the evaluated LF and the new corrected HF sub-bands are merged by applying the inverse DWT. A general astronomical image data set is picked out of the validation objective. The experimental results manifest the excellent outcomes of the newly suggested technique above the rest tested techniques.

1. INTRODUCTION

Image processing is very substantial in Astronomy, particularly with the modern progress in space exploration and the technological evolution of more strong and sound observatories with more robust telescopes. The employ of image processing in Astronomy alters from visibility of image detail and fine structure which are complicated to detect in the row data, locate the distance from earth, and detection and categorization of celestial objects [1]. Astronomical images play a significant part in profound space reconnaissance as they provide a fast trail to acquire planetary information [2]. The remote sensing astronomical images are unsurprisingly extraordinary for future research of stellar bodies [3]. However, the physical resolution of astronomical imaging devices such as space telescopes is restricted by system parameters (such as lens aperture and Charge-Coupled Device array characteristics) and physical effects (such as the atmosphere) [4]. Thus, observed images possibly manifest distorted thereby chosen for enhancement and then applied for visual estimate [5]. To increase the spatial resolution of celestial bodies, it is substantial to achieve resolution improvement techniques in order to recover the missing image details caused by the restrictions of imaging sensors [6].

The spatial resolution indicates the capability of the sensor to recognize the tiniest object depending on the pixel size [4]. The pixel numbers per unit area included in an image define the spatial resolution. If the pixel numbers per unit area are high this means that this image is HR image, and therefore it will consist of more detail [7]. The imaging devices initially determine the spatial resolution of a digital image. They contain an array of two-dimension photo-detector pixels. If the detector numbers are high, the spatial resolution probable of the imaging sensor will be high. An imaging device for incomplete detector numbers will generate an LR image [8]. Enhancing resolution primarily focuses on obtaining the HR image from the observed LR image. It uses either a single LR image [9, 10] or many LR images, which is known as super-resolution (SR) [11]. It has been quite an effective area of research for many applications, such as astronomical observation [1-6], satellite imaging [10, 12], medical diagnostics [13], and video surveillance systems [14].

A most related technique to image resolution enhancement is image interpolation, which is also employed to boost the pixel numbers in an image. Fundamentally, it endeavours to assess pixels at unknown positions utilizing known pixels [15]. There are four linear conventional interpolation techniques. Although linear techniques are used to improve spatial

resolution, they cannot process the rapid-increasing statistics around edges and accordingly result in blurred edges and unwanted artifacts. Other nonlinear interpolation techniques which are called edge-directed (EDI) and new edge- directed interpolation (NEDI) [16, 17], have been presented to substantially enhance the visible goodness of the pixels near edges by considering edge information into account. However, the enhancements using these techniques are restricted in the textile as well as not linear edges of the reconstructed images [18].

Wavelet-based is another resolution enhancement technique that is capable of supplying frequency and temporal information together at the transformation operation, and merging features of both [19]. The wavelet transform (WT) is based on splitting involved data into various frequency bands and thereafter inspects every one through a corresponding resolution at its scale [20]. The idea beyond the technique of wavelet transformation of an image is that image features in various scales are deposed and studied. Global features are studied at coarser scales, whereas local features are resolved at smooth scales [21]. The wavelet transform relies on small waves defined as wavelets, that are differing in frequency and limited in duration [22]. The based functions which are called Wavelets resulted from the single mother function by employing the shifts and expansions merit [23].

Many methods for image resolution enhancement have been performed by modeling the high-frequencies of sub-bands using detailed wavelet coefficients. The simplest method is named wavelet zero padding (WZP), in which a first evaluation of unknown HR image was acquired in two steps: Firstly, employing LR image as an input instead of the LF sub-band together with zero-padding for all sub-bands of HF elements; secondly, performing the inverse wavelet transform (IWT). The WZP technique inserts artifacts like blurring and ringing into the resolution enhanced image [24]. A cycle-spinning (CS) method, presented by Temizel and Vlachos [24], succeeded in decreasing ringing artifacts. In this method, many LR images were generated from HR one by spatially directional translations, wavelet transformation, dismissing the sub-bands of high-frequencies, and then performing WZP to all these LR images and taking the average to those middle HR images to get the ultimate enhanced image. Recently, there were many studies conducted on applying DWT for image enhancement. One-level DWT was employed by Tsai and Acharya [25], for dividing an LR image into frequency of quadratic sub-bands, and thereafter high-frequencies (LH) with (HL) were up-scaled by introducing zeros between sequential columns as well as rows, and (HH) was dismissed. Finally, the IDWT was applied to those estimated sub-bands to create the up-scaled HR image. Recently, the authors Demirel and Anbarjafari proposed (DASR) method [26], based on employing a bicubic method for interpolating input images with the pre-divided sub-bands of LH, HL, and HH. DWT and difference image (DWT-Diff) method was introduced by Demirel and Anbarjafari [27], for further improving the interpolated HF bands, the distinction between the estimated LL band and the LR image was applied, and appending the distinction to the evaluated sub-bands. The same authors also introduced a DWT and SWT (DWT-SWT) method [28], depended on using the same interpolating technique of sub-bands (LH, HL, and HH) with the input image by utilizing bicubic and rectifying the evaluated sub-bands through SWT. However, the enhancements by these considered methods have restricted performance due to their employed interpolation methods and they are not able to address the noise artifacts in the LR image observation.

This work presents a new approach that is based on merging SWT with DWT and NEDI to improve spatial accuracy and retrieving the missing edges due to the restrictions of imaging devices. The objective of this paper is to enhance the goodness of astronomical images so that the reconstructing images are more appropriate than the row ones for briefing of attributes. The implementation of the suggested method is particularly useful when a scene is acquired by a LR imaging sensor with an insufficient number of detector elements.

This paper concentrates its application on astronomical images although the proposed method also applies to all kinds of images, this is because row astronomical images usually contain noise and blur, thus, they cannot be used directly in analysis and research. This paper is ordered as follows. Section 2 elucidates the suggested approach. Five tested astronomical images are applied in Section 3 for the results and discussions. Section 4 shows the conclusions.

2. PROPOSED RESOLUTION ENHANCEMENT APPROACH

Recovering the edges involved in an observed image which are missing due to the restrictions of imaging devices, is the fundamental objective to retrieve the HR image from the perceived LR image. Although the conventional interpolation techniques addressed the dilemma of the retrieving process, they output blurring concerning edge regions as the pertinent data of edges in the row image are neglected.

Thus, the wavelet-based accuracy amendment technique is performed to maintain the edge details and accordingly recover the enhanced image from the observed image. In the suggested approach, the decomposition of sub-bands for HF was implemented by employing the DWT to separate and maintain the elements of high frequency, afterward implementing the interpolation of separated high-frequencies with the aim of maintaining better image details in comparison to direct interpolation. Although the combination of DWT process with the interpolation methods was applied in some of the DWT-based interpolation methods, the blurring impact from their use of conventional interpolation techniques gives rise to the prospective luck of edges in the estimated sub-bands. Thus, the NEDI method [17] was employed to be merged with DWT based on our approach DWT-NEDI in reference [10] that preserved more edges in the interpolating coefficients.

The proposed paper presents a new wavelet-based approach which is based on combining the techniques of SWT, DWT, NEDI together with soft thresholding. The proposed approach works for retrieving the wasted HF details and addressing the noise artifacts for the given noisy LR image. The justification behind choosing these specific techniques is that DWT supplies appropriate details for local analysis and image composition. It is able to give analysis for image information of different resolutions; smooth resolution comprises items of small size or low contrast, whereas rough resolution contains all items of large size or high contrast [23]. The rationale for selecting the NEDI is that it comes with estimating the wasted pixel via performing a weighted average which is basically applied on the four nearest adjacent pixels via diametrical direction [17]. The rationale for choosing the SWT is to further amending the detailed wavelet coefficients. The benefit of

using DWT with NEDI is to improve the visual quality of the reconstructed image. This feature cannot be obtained using the NEDI method separately. There are four main steps in the suggested approach. First, the DWT operation is applied to divide the LR image into four directional sub-bands ("LL, LH, HL, and HH") of low and high-frequencies (LF and HF) respectively. Because of the downsampling process is exploited in DWT process. DWT is shift-variant accordingly each sub-band comes with half the size of the given image. Second, NEDI technique is used to interpolate three HF sub-bands of LH, HL, and HH with a scale factor of $\alpha/2$. On the other hand, further enhancement is achieved for evaluated wavelet coefficients, the SWT process is introduced by dividing the orignal image into low and high sub-bands. Then, appending the LH, HL, and HH high sub-bands obtianed from SWT to the estimated DWT HF sub-bands. The SWT is not capable of downsampling, thus each sub-band comes with the full size of the original image. Third, NEDI method by $\alpha/2$ can be employed further to the rectified sub-bands. Generally, astronomical data acquired from imaging sensors are messy and noisy (e.g., additive Gaussian noise). Thus, to protect more edges and suppress the noise in the corrected wavelet coefficients, an adaptive thresholding process by an adaptive soft-thresholding method presented by Donoho [29] and Zhang [30] is included to handle the modified coefficients. Global threshold τ for sub-band is calculated by:

$$\tau = \sigma\sqrt{2\log(N)/N} \tag{1}$$

where, σ is the standard deviation, and N stands for number of total pixels. Soft-thresholding function is apparently presented as follow:

$$X_{out}(i,j) = \begin{cases} X_{in}(i,j) - \tau & X_{in}(i,j) > \tau \\ 0 & |X_{in}(i,j)| \le \tau \\ X_{in}(i,j) + \tau & X_{in}(i,j) < -\tau \end{cases} \tag{2}$$

The adaptive thresholding implementation process depends on concentrating the signal energy on little coefficients whilst spreading the noise energy among all wavelet coefficients [30].

Fourth, the resulting LL sub-band of DWT operation is substituted as LR image input because it includes additional data in comparison to the LL sub-band. To interpolate the LR image, the NEDI method by α/2 is applied and then substituted by the evaluated LL sub-band. Ultimately, the operation of IDWT is implemented to produce a reconstructed image by merging the evaluated LF with the new HF sub-bands. The below figure depicts the proposed DWT-NEDI-SWT technique is shown by Figure 1.

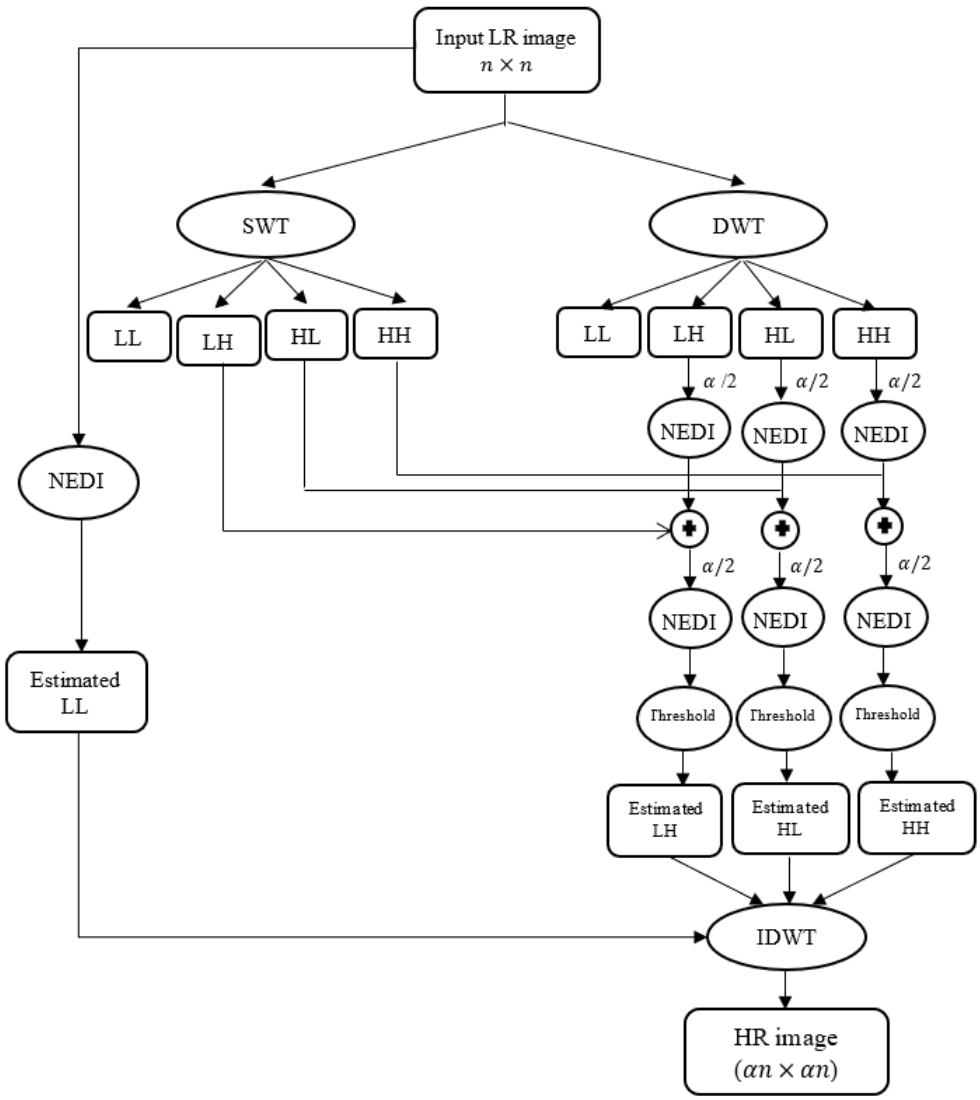

Figure 1. Block diagram of the proposed resolution technique

The distinct processing steps can be illustrated in a separate manner as follows:

(1) Red component selection from the observed color image.

(2) Performing DWT procedure for splitting the selected component into four sub-bands of low and high frequencies with half the size of the original image.

(3) Applying NEDI technique by scale factor α/2 for upsampling the high (LH, HL, and HH) sub-bands due to the downsampling that is caused by DWT.

(4) Performing SWT operation for separating the adopted component into four low and high sub-bands with full size. Given that SWT is not coming with downsampling.

(5) Appending the high sub-bands of SWT with the interpolated high sub-bands of DWT for further amending of these estimated sub-bands.

(6) Applying again the NEDI by α/2 for upsampling these rectified sub-bands to maintain extra edges.

(7) Performing an adaptive thresholding procedure after calculating the threshold of any sub-band for suppressing the noise at these rectified sub-bands.

(8) Employing the NEDI by scale factor α/2 for upsampling the examind LR image to generate the evaluated low sub-band of LL.

(9) Performing IDWT procedure for merging all handled sub-bands and getting enhanced components.

(10) Blue and green components are identically generated by employing steps 2 to 9.

(11) Merging the resultant handled components for getting the upgraded HR color image.

3. RESULTS AND DISCUSSIONS

3.1 Visual evaluation

The experimental results will be thoroughly displayed in this section. The output visual implementation for both the proposed technique and the other studied amendment techniques will be discussed. The proposed technique was implemented upon five various astronomical images called Cats Eye Nebula, Dark Matter Galaxy, Orion Nebula, Centaurus Galaxy, and Jupiter Planet acquired from an astronomical general data set. Because the scale for the row HR images in the general data set is varied, thus, each row image was up-sampled to 512×512 pixels and it was considered as the reference image for the consistency of comparison. Depending on the observation of imaging devices, the measured LR images were generated with the scale of 128×128 pixels as follows: the row images are blurred using a filter of low-pass, and then down-sampled in the vertical orientation as well as in the horizontal orientation with a scale factor α by employing twice DWT based on the (db.9/7) wavelet function. Gaussian noise is used for contaminating the produced LR images based on 40 dB of signal-to-noise ratio (SNR). The advantage of choosing the wavelet Daubechies db.9/7 is that because it is the best wavelet filter for the dividing process using DWT [31].

To appreciate the visual implementation of the output results, three images called Orion Nebula, Centaurus Galaxy, and Jupiter Planet were picked out from five images that were tested by the proposed algorithm and the other considered algorithms. Figures 2-4 display the reconstructed images generated from all tested techniques through a resolution enhancement from 128 × 128 to 512 × 512 for the selected images. It has been noticed that the suggested approach demonstrates a preferable visual quality to the other tested approaches in improving the input LR images by providing more detail of interested regions and removing the noise artifacts.

The detail of the chosen reconstructed regions of Orion Nebula and Centaurus Galaxy images produced by the suggested approach, for instance, are frequently spotless, in comparison with the reconstructed regions of these images resulted from the other considered techniques. In addition, the local features, such as edges and surface textures of the improved areas of these images obtained by the proposed algorithm are obviously distinct in comparable with the other tested methods. Furthermore, the noise and ringing effects are eliminated by the suggested technique. For example, the ringing and noise artefacts at the reconstructed region of Jupiter planet image are removed ultimately by the suggested algorithm, whilst these artefacts are manifested plainly at the images resulted from the other techniques.

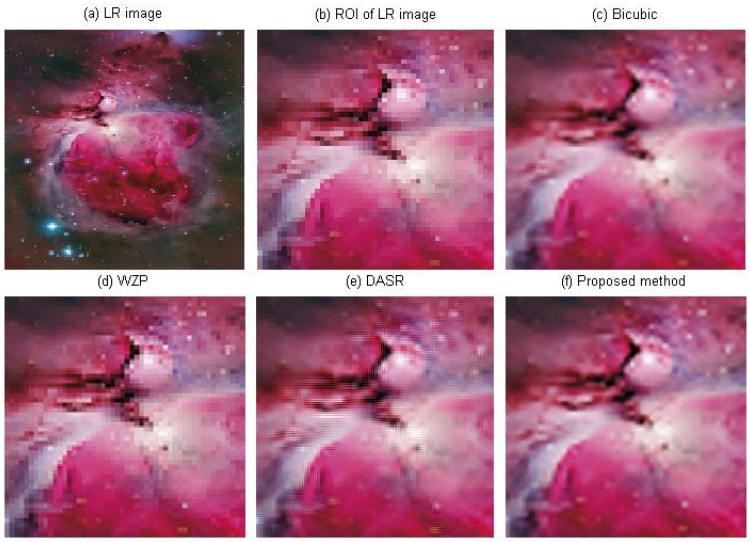

Figure 2. The reconstructed images produced by up-sampling of 128 × 128 to 512 × 512 with proposed technique and the other tested techniques for an Orion Nebula selected image. (a) the full LR image; (b) the chosen area from LR image; the reconstructed HR images using (c) Bicubic, (d) WZP, (e) DASR and (e) the suggested technique

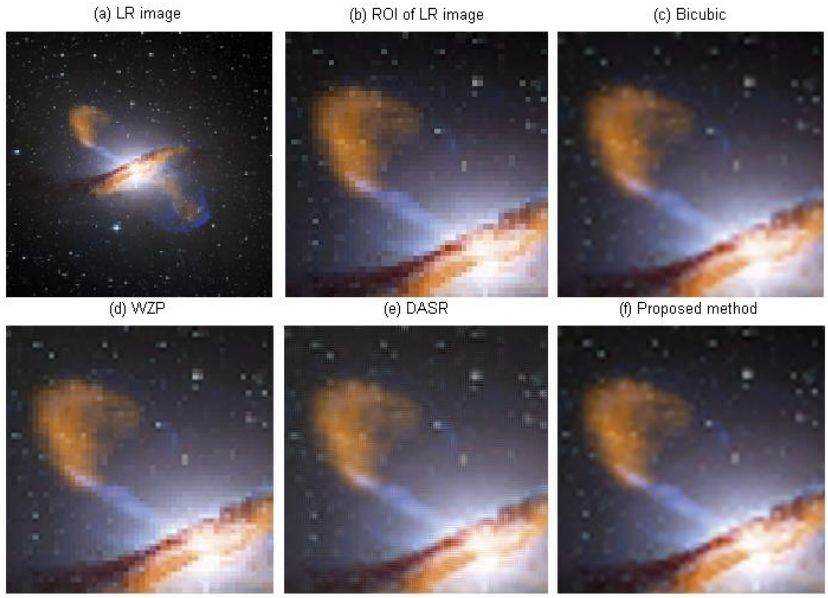

Figure 3. The reconstructed images produced by up-sampling of 128 × 128 to 512 × 512 with proposed technique and the other tested techniques for a Centaurus Galaxy selected image. (a) the full LR image; (b) the chosen area from LR image; reconstructed HR images using (c) Bicubic, (d) WZP, (e) DASR and (e) the suggested technique

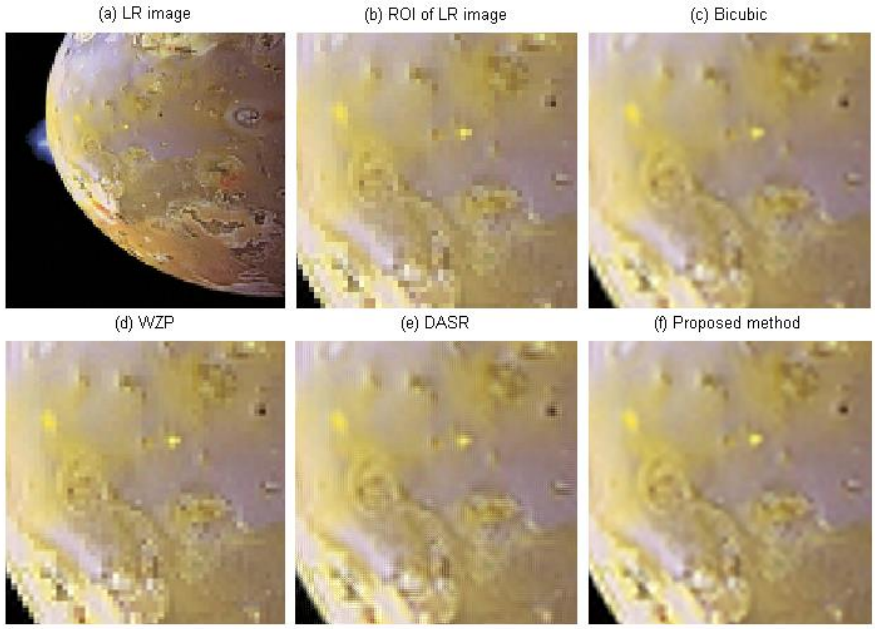

Figure 4. The reconstructed images produced by up-sampling of 128 × 128 to 512 × 512 with proposed technique and the other tested techniques for a Jupiter Planet selected image. (a) the full LR image; (b) the chosen area from LR image; reconstructed HR images using (c) Bicubic, (d) WZP, (e) DASR and (e) the suggested technique

3.2 Quantitative evaluation

As it is difficult to assess visually the distinction between the reconstructed images from various techniques because this difference can be little. This segment shows the experimental outcomes of the objective evaluation. Peak-signal-to-noise-ratio (PSNR) between the enhanced and the row HR images is used, because it is the maximum ordinarily quantitative measure for assessing image goodness. It is computed as:

$$PSNR = 10\log_{10}(\frac{L^2}{MSE}) \quad (3)$$

where, L is the highest value at the image. The value of L will be 255 if the image is presented with 8-bit grayscale. MSE is the mean-square-error of the reconstructed $\hat{X}(i,j)$ and the row $X(i,j)$ images. It is computed as:

$$MSE = \frac{1}{N \times N}\sum_{i=1}^{N}\sum_{j=1}^{N}\left[\hat{X}(i,j) - X(i,j)\right]^2 \quad (4)$$

The second commonly quantitative measure is root-mean-square error (RMSE) [14], and it is expressed as:

$$RMSE = \sqrt{MSE} \quad (5)$$

As the error images for considered methods are quite approaching to each other and it is so tricky to do evaluation,

entropy is the commonly used quantitative measure for evaluating image quality. The entropy of an image, indicated by E, can be expressed by:

$$E = -\sum_{k=1}^{L} P(r_k) log_2 P(r_k) \quad (6)$$

where, $P(r_k)$ is the likelihood of a brightness value r_k. The lower the E value, the better the amendment, according to Azam et al. [32].

Table 1. The PSNR (dB) outcomes of 128×128 to 512×512 enlargement within the chosen images

Techniques	Types of Images				
	Cats	**Dark**	**Orion**	**Centaurus**	**Jupiter**
Nearest	32.02	26.81	26.34	27.33	26.05
Bilinear	33.61	28.00	27.48	28.22	27.13
Bicubic	33.58	28.02	27.43	28.15	27.25
Lanczos	33.51	27.97	27.35	28.09	27.24
WZP [22]	34.27	28.51	27.97	28.51	27.32
WZP-CS [22]	35.71	29.59	28.86	29.11	28.15
DWT [23]	34.15	28.37	27.85	28.42	27.20
DASR [24]	34.49	27.96	27.37	28.00	26.79
DWT-Dif [25]	31.76	26.27	25.85	26.92	25.39
DWT-SWT [26]	33.27	27.22	26.41	27.36	25.79
DWT-NEDI [8]	36.58	27.72	28.18	25.87	26.35
Proposed method	**38.33**	**30.76**	**29.94**	**29.87**	**28.75**

Tables 1-3 respectively include the objective results of the chosen astronomical images. Depending on the PSNR and RMSE values, it has been perceived that the suggested method has the top implementation of the five picked images. It is illustrated that the suggested algorithm performs the maximum PSNR values (38.33 dB, 30.76 dB, 29.94 dB, 29.87 dB, and 28.75 dB for PSNR respectively) for all five tested images and the increment over DWT-NEDI algorithm is 5%, 11%, 6%, 16%, and 9%. Depending on the values of entropy, the proposed method has the maximum achievement for the *Cats Eye Nebula* and Centaurus Galaxy images, the DWT-NEDI method gives the maximum accomplishment for the *Dark Matter Galaxy* and *Jupiter Planet* images, while the superior method is the WZP for the Orion Nebula image. Notwithstanding, the suggested approach still has a superior performance better than the other studied techniques. These perceptions substantiate that the achievement of the proposed algorithm relies on the evaluation metrics and diverse image attributes. Table 4 presents the comparison of the proposed technique against the other methods based on the advantages and disadvantages of each method. Overall, the proposed technique performs better reconstruction quality than other methods in terms of subjective and quantitative metrics.

Table 2. The RMSE outcomes of 128×128 to 512×512 enlargement within the chosen images

Techniques	Types of Image				
	Cats	**Dark**	**Orion**	**Centaur**	**Jupiter**
Nearest	6.39	11.64	12.29	10.96	12.71
Bilinear	5.32	10.15	10.78	9.90	11.22
Bicubic	5.34	10.13	10.84	9.98	11.07
Lanczos	5.39	10.19	10.94	10.04	11.08
WZP [22]	4.93	9.57	10.18	9.57	10.97
WZP-CS [22]	4.18	8.46	9.20	8.93	9.97
DWT [23]	5.00	9.73	10.33	9.68	11.13
DASR [24]	4.81	10.20	10.92	10.15	11.67
DWT-Dif [25]	6.58	12.39	13.00	11.50	13.72
DWT-SWT [26]	5.53	11.11	12.19	10.93	13.09
DWT-NEDI [8]	3.78	10.49	9.95	12.97	12.28
Proposed method	**3.09**	**7.39**	**8.12**	**8.19**	**9.31**

Table 3. The Entropy outcomes of 128×128 to 512×512 enlargement within the chosen images

Techniques	Types of Images				
	Cats	**Dark**	**Orion**	**Centaurus**	**Jupiter**
Nearest	5.32	3.94	4.04	3.86	4.76
Bilinear	5.74	4.02	3.95	3.88	5.04
Bicubic	5.73	4.05	3.96	3.96	5.03
Lanczos	5.73	4.10	4.01	4.04	5.04
WZP [22]	5.42	3.99	4.06	3.92	4.75
WZP-CS [22]	5.84	3.93	**3.91**	3.87	5.24
DWT [23]	5.40	4.01	4.07	3.96	4.77
DASR [24]	5.57	4.25	4.19	4.10	5.20
DWT-Dif [25]	5.46	3.86	4.10	4.22	5.00
DWT-SWT [26]	5.52	4.09	4.29	4.15	4.82
DWT-NEDI [8]	5.04	**3.66**	4.03	3.75	**4.34**
Proposed method	**5.03**	3.87	4.78	**3.69**	4.55

Table 4. The comparison of the proposed approach against the considered techniques

Resolution Enhancement Techniques	Advantages	Disadvantages
Convolution Interpolation	Simple to perform	Result in blurred edges and unwanted artifacts
WZP [22]	Easy to implement	Inserts smoothing and ringing effects
WZP-CS [22]	Decreases ringing effects	
DWT [23]	Insulates and maintains the HF components	Causes down sampling
DASR [24]	Insulates the detailed coefficients	Produces blurring around edge areas
DWT-NEDI [8]	Enhances the visual quality around edge areas and addresses noise artifacts	
Proposed	Preserves more detailed components, obtains better visual quality, and suppresses noise	

3.3 Variation of noise levels

This part demonstrates the power of the suggested approach versus noise artifacts depending on the adaptive thresholding process. The principal concept of this process is concentrating the signal energy on a little bigger coefficient whilst spreading the noise energy among all coefficients. Thus, the adaptive thresholding process heads for preserving bigger coefficients

and compressing noise coefficients. The noise level has been raised from 40 to 20 (dB) of 5 dB increment. The first image has been tested using the suggested algorithm and other selected algorithms. Table 5 illustrates the PSNR outcomes comparison of various algorithms with several levels of noise. It has been noticed that the suggested approach results the best PSNR results among the selected methods for every noise level.

Table 5. The PSNR results of the Cats Eye Nebula image for different noise levels, rise from 20 dB to 40 dB with an increment of 5 dB

SNR	Techniques				
	Nearest	**Bilinear**	**Lanczos**	**Bicubic**	**Proposed**
40 dB	32.02	33.61	33.51	33.58	38.29
35 dB	31.65	33.36	33.08	33.22	37.45
30 dB	30,71	32.74	32.05	32.32	35.53
25 dB	28.59	31.20	29.80	30.28	32.22
20 dB	25.10	28.20	26.17	26.81	27.95

4. CONCLUSIONS

A developed wavelet-based approach depended on a merging of three algorithms which are stationary wavelet transform, discrete wavelet transform, and new edge-directed interpolation was proposed in this research to enrich the spatial resolution via retrieving the edges for an observed low-resolution image. A soft-thresholding operation is also introduced for maintaining more edges and suppressing the noise in the wavelet coefficients of the astronomical noisy low-resolution image improvement. The novelty of this method is the combination of stationary wavelet transform and a thresholding process to rectify the estimated noisy wavelet coefficients. The implementation of this method is particularly beneficial when a scene is captured by a low-resolution imaging device with an insufficient number of detector elements. Five types of astronomical images were selected and examined via the suggested algorithm, and the experimental results were tested with interpolation techniques and wavelet-based image techniques. Results have indicated that the proposed technique overcomes the examined resolution enhancement techniques.

ACKNOWLEDGMENT

A great gratitude to the Iraqi Ministry of Higher Education and Scientific Research for continued upholding and encouragement. This paper is funded by Ministry of Higher Education and Scientific Research in Iraqi.

REFERENCES

[1] Misra, D., Mishra, S., Appasani, B. (2018). Advanced image processing for astronomical images.arXiv preprint arXiv:1812.09702. https://doi.org/10.48550/arXiv.1812.09702

[2] Zhang, J., Wang, F., Zhang, H., Shi, X. (2023). A Novel CS 2G-starlet denoising method for high noise astronomical image. Optics & Laser Technology, 163: 109334. https://doi.org/10.1016/j.optlastec.2023.109334

[3] Zhang, Y., Jiang, J., Zhang, G. (2021). Compression of remotely sensed astronomical image using wavelet-based compressed sensing in deep space exploration. Remote Sensing, 13(2): 288. https://doi.org/10.3390/rs13020288

[4] Yue, L., Shen, H., Li, J., Yuan, Q., Zhang, H., Zhang, L. (2016). Image super-resolution: The techniques, applications, and future. Signal Processing, 128: 389-408. https://doi.org/10.1016/j.sigpro.2016.05.002

[5] Alasta, A.F., Algamudi, A., Qahwaji, R., Ipson, S., Hauchecorne, A., Meftah, M. (2019). New method of enhancement using wavelet transforms applied to SODISM telescope. Advances in Space Research, 63(1): 606-616. https://doi.org/10.1016/j.asr.2018.08.002

[6] Li, Z., Peng, Q., Chen, Y., Zhang, Q., Wang, N. (2018). Image resolution enhancement techniques for galaxy images. AIP Conference Proceedings, 1955(1): 040153. https://doi.org/10.1063/1.5033817

[7] Park, S.C., Park, M.K., Kang, M.G. (2003). Super-resolution image reconstruction: A technical overview. IEEE Signal Processing Magazine, 20(3): 21-36. https://doi.org/10.1109/MSP.2003.1203207

[8] Nasrollahi, K., Moeslund, T.B. (2014). Super-resolution: a comprehensive survey. Machine Vision and Applications, 25: 1423-1468. https://doi.org/10.1007/s00138-014-0623-4

[9] Witwit, W., Zhao, Y., Jenkins, K.W., Zhao, Y. (2016). An optimal factor analysis approach to improve the wavelet-based image resolution enhancement techniques. Global Journal of Computer Science and Technology: F Graphics & Vision, 16(3): 11-20.

[10] Witwit, W., Zhao, Y., Jenkins, K., Zhao, Y. (2017). Satellite image resolution enhancement using discrete wavelet transform and new edge-directed interpolation. Journal of Electronic Imaging, 26(2): 023014. https://doi.org/10.1117/1.JEI.26.2.023014

[11] Witwit, W., Zhao, Y., Jenkins, K., Addepalli, S. (2018). Global motion based video super-resolution reconstruction using discrete wavelet transform. Multimedia Tools and Applications, 77: 27641-27660. https://doi.org/10.1007/s11042-018-5941-5

[12] Zhang, H., Yang, Z., Zhang, L., Shen, H. (2014). Super-resolution reconstruction for multi-angle remote sensing images considering resolution differences. Remote Sensing, 6(1): 637-657. https://doi.org/10.3390/rs6010637

[13] Robinson, M.D., Chiu, S.J., Toth, C.A., Izatt, J.A., Lo, J.Y., Farsiu, S. (2017). New applications of super-resolution in medical imaging. In Super-Resolution Imaging, pp. 383-412.

[14] Zhang, L., Zhang, H., Shen, H., Li, P. (2010). A super-resolution reconstruction algorithm for surveillance images. Signal Processing, 90(3): 848-859. https://doi.org/10.1016/j.sigpro.2009.09.002

[15] Witwit, W., Zhao, Y., Hallawi, H. (2024). Wavelet-based spatial resolution enhancement for thermal images. Ingenierie des Systemes d'Information, 29(5): 1679-1686. https://doi.org/10.18280/isi.290502

[16] Allebach, J., Wong, P.W. (1996). Edge-directed interpolation. In Proceedings of 3rd IEEE International Conference on Image Processing, Lausanne, Switzerland, pp. 707-710. https://doi.org/10.1109/ICIP.1996.560768

[17] Li, X., Orchard, M.T. (2001). New edge-directed interpolation. IEEE Transactions on Image Processing,

10(10): 1521-1527. https://doi.org/10.1109/83.951537
[18] Tam, W.S., Kok, C.W., Siu, W.C. (2010). Modified edge-directed interpolation for images. Journal of Electronic Imaging, 19(1): 013011. https://doi.org/10.1117/1.3358372
[19] Crouse, M.S., Nowak, R.D., Baraniuk, R.G. (1998). Wavelet-based statistical signal processing using hidden Markov models. IEEE Transactions on Signal Processing, 46(4): 886-902. https://doi.org/10.1109/78.668544
[20] Daubechies, I. (1992). Ten Lectures on Wavelets. Society for Industrial and Applied Mathematics.
[21] Nguyen, N., Milanfar, P. (2000). A wavelet-based interpolation-restoration method for superresolution (wavelet superresolution). Circuits, Systems and Signal Processing, 19: 321-338. https://doi.org/10.1007/BF01200891
[22] Bhandari, A.K., Soni, V., Kumar, A., Singh, G.K. (2014). Cuckoo search algorithm based satellite image contrast and brightness enhancement using DWT–SVD. ISA Transactions, 53(4): 1286-1296. https://doi.org/10.1016/j.isatra.2014.04.007
[23] Mallat, S.G. (1989). A theory for multiresolution signal decomposition: The wavelet representation. IEEE Transactions on Pattern Analysis and Machine Intelligence, 11(7): 674-693. https://doi.org/10.1109/34.192463
[24] Temizel, A., Vlachos, T. (2005). Wavelet domain image resolution enhancement using cycle-spinning. Electronics Letters, 41(3): 1.
[25] Tsai, P.S., Acharya, T. (2006). Image up-sampling using discrete wavelet transform. In 9th Joint International Conference on Information Sciences (JCIS-06). https://doi.org/10.2991/jcis.2006.340
[26] Anbarjafari, G., Demirel, H. (2010). Image super resolution based on interpolation of wavelet domain high frequency subbands and the spatial domain input image. ETRI Journal, 32(3): 390-394. https://doi.org/10.4218/etrij.10.0109.0303
[27] Demirel, H., Anbarjafari, G. (2011). Discrete wavelet transform-based satellite image resolution enhancement. IEEE Transactions on Geoscience and Remote Sensing, 49(6): 1997-2004. https://doi.org/10.1109/TGRS.2010.2100401
[28] Demirel, H., Anbarjafari, G. (2010). Image resolution enhancement by using discrete and stationary wavelet decomposition. IEEE Transactions on Image Processing, 20(5): 1458-1460. https://doi.org/10.1109/TIP.2010.2087767
[29] Donoho, D.L. (1995). De-noising by soft-thresholding. IEEE Transactions on Information Theory, 41(3): 613-627. https://doi.org/10.1109/18.382009
[30] Zhang, X.P. (2001). Thresholding neural network for adaptive noise reduction. IEEE Transactions on Neural Networks, 12(3): 567-584. https://doi.org/10.1109/72.925559
[31] Skodras, A., Christopoulos, C., Ebrahimi, T. (2001). The JPEG 2000 still image compression standard. IEEE Signal Processing Magazine, 18(5): 36-58. https://doi.org/10.1109/79.952804
[32] Azam, S., Zohra, F.T., Islam, M.M. (2014). A state-of-the-art review on wavelet based image resolution enhancement techniques: performance evaluation criteria and issues. International Journal of Image, Graphics and Signal Processing, 6(9): 35-46. https://doi.org/10.5815/ijigsp.2014.09.05